Gain, Noise Figure and Bandwidth-Limited Dynamic Range of a Low-Biased External Modulation Link

Harold V. Roussell, Michael D. Regan, Joelle L. Prince, Charles H. Cox, Jianxiao X. Chen, William K. Burns, Gary E. Betts, and Edward I. Ackerman
Photonic Systems, Inc.
Billerica, Massachusetts, USA

Joe C. Campbell
School of Engineering and Applied Science
Department of Electrical and Computer Engineering
University of Virginia
Charlottesville, Virginia, USA

***Abstract*—We present a broad-bandwidth (1 – 12 GHz) low-biased external modulation fiber-optic link without pre-amplifiers that has a gain of 6 dB – 14 dB and a noise figure of < 7.5 dB everywhere in this broad bandwidth, with a record low noise figure of only 3.4 dB at 2 GHz. The third-order distortion-limited spurious-free dynamic range (*SFDR*) of this link within any suboctave portion of the 1 – 12 GHz range of operating frequencies is approximately 120 dB·Hz$^{2/3}$ in a 1-Hz instantaneous receiver bandwidth. We describe the high-performance components in this link and discuss the extent to which their performance varies with frequency, and show which of these components' frequency-dependent parameters affect which of the three figures of merit (gain, noise figure, and *SFDR*).**

I. Introduction

In sensing systems that employ analog fiber-optic links for signal remoting, the noise figure of these links dictate the system's sensitivity to received signals. The demonstration of an intrinsic link—which we define as a link that uses no electronic amplifiers—that exhibits a broadband noise figure comparable to that of commercial broadband low-noise amplifiers (LNAs) has represented a "holy grail" for analog link designers. The external modulator in such a link can connect directly to a receiving antenna, and its optimum bias voltage can be maintained by a small circuit at this location that consumes only a few milliwatts of dc power. The other required link components — a high-power, low-relative-intensity-noise (low-*RIN*) optical source and a high-speed photodetector — can reside near the system receiver(s) for easier maintenance.

The first reports of intrinsic analog fiber-optic links with measured noise figures of < 10 dB, and with correspondingly high dynamic ranges, used *passive* resonant circuits at the link input to mimic the effect of *active* pre-amplification with an LNA – albeit only over narrow bandwidths (≤ 10%) at the rather low frequencies (~ 100 MHz) where it was possible to realize highly resonant input impedance matching circuits [1, 2]. With the advent of higher-power optical sources and lower-V_π electro-optic modulators, some researchers have more recently broken the 10-dB noise figure barrier over bandwidths of an octave or more at frequencies > 1 GHz (and in some cases at frequencies up to 12 GHz) using differential-detection [3, 4] or low-biased [4, 5] external modulation link architectures.

In this paper, we report the lowest measured noise figure for a broad-bandwidth 1 – 12 GHz intrinsic optical link and a measured spurious-free dynamic range (*SFDR*) that is correspondingly high but is limited by an unavoidable feature of the low-biasing architecture to a suboctave portion of that potential 12:1 bandwidth. As has been reported previously [4], the devices used in this link can also be used in configurations suitable for multi-octave operation such as the balanced detection architecture.

For an intrinsic low-biased external modulation link there are three components with frequency-dependent performance characteristics:

1) a p-i-n photodiode detector with a large photosensitive region (diameter = 34 μm) that facilitates coupling from the optical fiber but contributes to the substantially frequency-dependent gain for the intrinsic link.
2) a Mach-Zehnder electro-optic modulator with very long electrodes (~ 14 cm) that minimize V_π at low frequencies but generally yield performance that is more frequency-dependent than that of modulators with shorter electrodes; the dual-drive electrode configuration of this modulator reduces its V_π but also in turn requires use of:
3) a commercial hybrid coupler with its own frequency-dependent behavior.

In section II of this paper we describe a link we assembled from these components, and in section III we show how their frequency-dependent behaviors in turn dictate the frequency dependence of the link's gain, noise figure, and *SFDR*.

This material is based upon work supported by DARPA under SSC-San Diego Contract No. N66001-04-C-8045. Any opinions, findings and conclusions or recommendations expressed in this material are those of the authors and do not necessarily reflect the views of DAPRA or SSC San Diego.

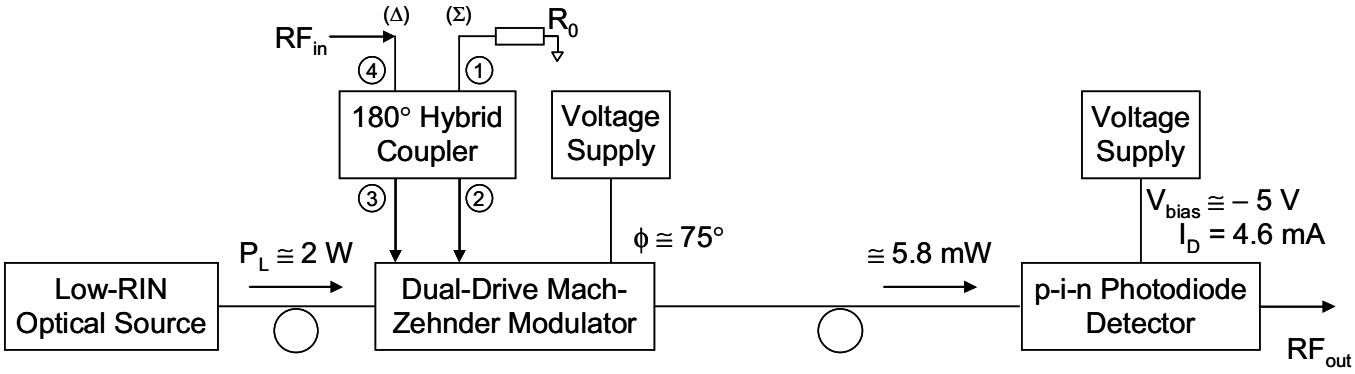

Fig. 1 Block diagram of the link using a low-biased dual-drive Mach-Zehnder modulator.

II. Link Description

Figure 1 shows a block diagram of the link that we assembled for the purposes of this investigation.

The optical source consisted of a 150-mW fiber laser oscillator that we followed with an Erbium-doped fiber amplifier to create a master-oscillator power amplifier (MOPA) with > 3 W of 1.55-μm optical power coupled into polarization-maintaining single-mode fiber. With careful engineering of this MOPA, we obtained a substantially frequency-independent *RIN* ≈ –172 dB/Hz at all frequencies > 1 GHz. Because low biasing reduces the average optical power incident on the photodiode detector, and because the MOPA's *RIN* was so low, *RIN* as a whole had a negligible effect on the noise figure of the link depicted in Fig. 1.

The detector we used was fabricated using a 34-μm-diameter rear-illuminated partially-depleted absorber design by the University of Virginia [6, 7]. Using RF probes to characterize this device, we found that it had a low-frequency fiber-coupled responsivity of ~0.8 A/W and could withstand illumination of > 80 mW. (This impressive power-handling capability, while not a necessary element of the low-biased link, is required for high *SFDR* in broadband, quadrature-biased Mach-Zehnder modulator-based links [3, 4].) We could therefore expect that the frequency response of this high-power device at the 5.8-mW illumination level indicated for the low-biased link in Fig. 1 would closely resemble that which we measured at the ~ 1 mW of modulated optical power output from an Agilent 8703B Lightwave Component Analyzer, which is shown in Fig. 2 (a).

The modulator in the link was a Mach-Zehnder with a Y-fed balanced-bridge (YBBM) optical waveguide pattern and dual-drive electrodes on z-cut $LiNbO_3$ designed by Photonic Systems, Inc. Devices fabricated in the dual-drive z-cut configuration exhibit lower V_π's than single-drive devices with the same electrode length on x-cut $LiNbO_3$. The optical waveguides in the modulator were made to interact with the imposed electrical field over a length of nearly 14 cm, and therefore the measured optical insertion loss was rather high at 7.8 dB but the measured V_π was a record low for a broad-bandwidth modulator: 0.93 V at 1 GHz and < 1.4 V at 12 GHz. To facilitate comparison to the gain and noise figure, in Fig. 2 (b) we have plotted $\pm 10 \cdot \log[V_\pi^2]$ in $dB \cdot V^2$.

It is important to note that the V_π we refer to here is that which one would measure through an "ideal" 180-degree hybrid coupler; *i.e.*, it is the voltage that must be supplied at the RF input port in Fig. 1 to switch the optical output of the modulator from maximum to minimum, assuming the coupler behaved ideally – with perfect amplitude balance and a 180-degree phase difference between ports 2 and 3 at all frequencies, and with no excess loss.

Fig. 2 (c) shows what we call the "ideality" factor of the hybrid coupler used in the link, which is a frequency-dependent quantity that expresses how much more readily the voltage difference between the two outputs of an "ideal" hybrid coupler modulates the light when a given signal is input at the Δ port than when the same signal is input at the Δ port of the actual hybrid. This voltage ratio is $\sqrt{2} \div |S_{34} - S_{24}|$, which is equal to 1 in an "ideal" coupler because in that case $S_{34} = -S_{24}$ and $|S_{34}| = |S_{24}| = 1/\sqrt{2}$ [8]. The factor which affects the link's gain and noise figure, and therefore the quantity plotted in Fig. 2 (c) as a function of frequency (along with its inverse), is actually the square of this voltage ratio, which varied from ~ 0.4 dB at 1 GHz to ~ 1.8 dB at 12 GHz.

III. Measured Link Performance Parameters and Their Frequency Response

Figure 2(d) shows the gain and noise figure of the link shown in Fig. 1, measured at 1-GHz intervals between 1 and 12 GHz.

We measured the gain shown by the blue points in Fig. 2(d) using an Agilent N5230A 4-port PNA Network Analyzer. Of the three measured link figures of merit it has the greatest dependence on frequency. Previously established link models [9, 10] explain that this is due to its dependence on all of the frequency-dependent parameters in the link: its proportionality to the detector's frequency response [shown in Fig. 2(a)], to the inverse of the square of the modulator's V_π [reflected in the $dB \cdot V^2$ quantity plotted in blue in Fig. 2(b)], and to the coupler's non-ideality [plotted in blue in Fig. 2(c)].

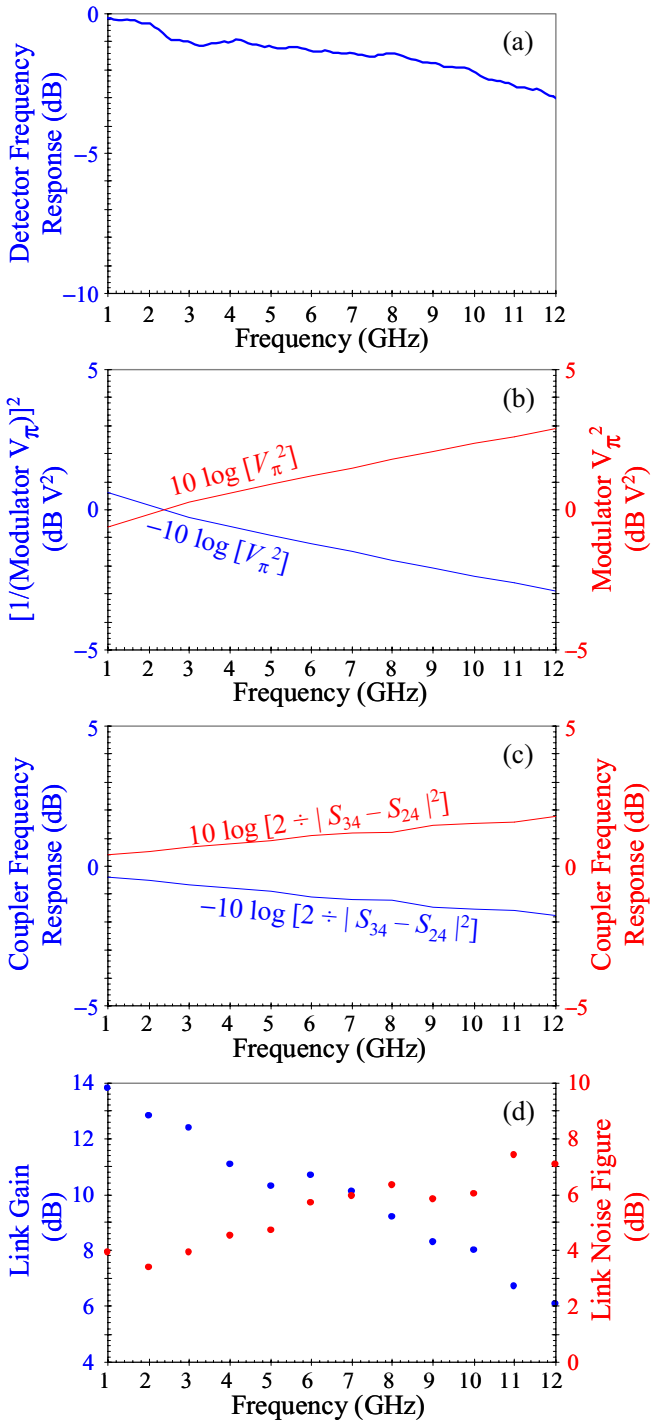

Fig. 2 Measured performance of the three link components with frequency-dependent parameters, and the resulting link performance.

(a) Frequency response (in dB) of the photodetector.
(b) ± 10·log [V_π^2] of the dual-drive Mach-Zehnder modulator if it were measured through an "ideal" 180-degree hybrid coupler.
(c) Measured "ideality factor" of the actual 180-degree hybrid coupler used in the experiment.
(d) Measured gain (blue points) and noise figure (red points) of the experimental link.

We have purposely plotted parts (a) – (d) of Fig. 2 all at the same scale, so that the dependence of the gain on the three frequency-dependent component parameters can be readily surmised. A quick glance shows that, across the 1 – 12 GHz band the detector frequency response dips by ~ 3 dB, the relevant measure of V_π (= – 10·log[V_π^2]) decreases by about 3.5 dB, and the coupler's "ideality" decreases by about 1.5 dB. The sum of these changes is the decrease in link gain of ~8 dB (from ~14 dB down to ~6 dB) between 1 GHz and 12 GHz.

Using a calibrated Agilent N8975A Noise Figure Analyzer, we also measured the noise figure shown in Fig. 2(d). To the author's knowledge, the measured noise figure of 3.4 dB at 2 GHz shown in this plot is the lowest ever reported for a broadband fiber-optic link without a pre-amplifier.

Noise figure is defined as the degradation of signal-to-noise ratio assuming an input noise arising only from thermal sources at a standardized temperature of $T_0 = 290$ K [11].

$$NF = 10 \log\left[\frac{\overline{n_{out}}}{kT_0 \cdot g_i}\right], \qquad (1)$$

where k is Boltzmann's constant, $\overline{n_{out}}$ is the link's output noise spectral density and g_i is its intrinsic gain. It has been shown previously [9, 10] that the dominant contributors to $\overline{n_{out}}$ are ones whose magnitudes are affected by the detector frequency response in the same way as the link's input signal is, but which unlike the signal are not influenced by the modulator's V_π. Nor would the dominant contributors to $\overline{n_{out}}$ depend in any way on the thermal noise generated in the hybrid coupler. Since g_i depends on all three of the frequency-dependent quantities listed at the end of section I, but $\overline{n_{out}}$ is proportional to only the detector response, the ratio in the brackets of (1), and thus the noise figure, should depend substantially on just the other two frequency-dependent quantities; i.e., it should be proportional to the square of the modulator's V_π and to the hybrid coupler's non-ideality, but independent of the detector's frequency response. Similarly to how we summed their effect on gain, if we sum the variations in the red curves of Fig. 2 (b) and (c), we get the ~ 5-dB variation in noise figure across the band shown in Fig. 2 (d).

Note that in [4] the authors reported lower noise figures at 6 – 12 GHz (4.4 dB – 5.8 dB) than what is shown at those frequencies in Fig. 2(e). This was due to our having used at that time a hybrid coupler optimized to have less than 0.6 dB of non-ideality across that octave-wide band, but which had poor performance at frequencies below 4 GHz. To enable measurements across a broader range of frequencies, for the link reported here we selected a coupler that sacrificed some overall ideality [see Fig. 2(c)] to enable generally good performance across the entire 1 – 12 GHz frequency range.

Fig. 3 shows the *SFDR* of the link, measured using a two-tone, third-order intermodulation distortion system designed by Photonic Systems, Inc. Error bars of ± 1 dB were deemed appropriate to the degree of uncertainty in measuring the very low-power 3rd-order intermodulation distortion products.

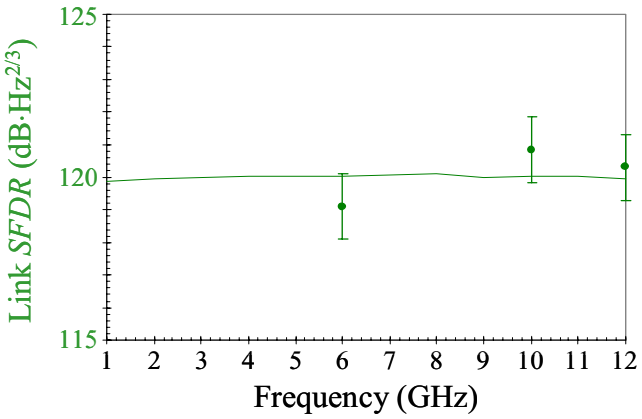

Fig. 3 Measured (points with ± 1-dB error bars) *SFDR* of the experimental link, and a curve showing the *SFDR* predicted by previously developed models [9, 10].

Notice from Fig. 3 that the *SFDR*, which can only be gleaned from a collection of many measured data points and whose determination is therefore much more time-consuming, was measured only at 6, 10, and 12 GHz. Because the measured *SFDRs* at those three frequencies closely correspond to what previously-developed analytical models predict [9, 10], we assume that we have correctly modeled the link's nonlinear behavior and that it would therefore also exhibit the predicted *SFDR* of ~ 120 dB·Hz$^{2/3}$ at lower frequencies if measured. There is very little change in the link's *SFDR* across 1 – 12 GHz because, like the output noise power density $\overline{n_{out}}$, in a link with modulator-dominated nonlinearity the output third-order intercept power is proportional to the detector frequency response and independent of both the modulator V_π and the hybrid coupler's behavior, and because the *SFDR* can be defined as [9]:

$$SFDR = \left(\frac{IP3_{out}}{\overline{n_{out}}} \right)^{\frac{2}{3}}. \qquad (2)$$

The modulator low-biasing technique that enabled us to achieve very low noise figures and therefore high *SFDR* across the 1 – 12 is not a frequency-dependent architecture *per se*; however second-order distortion generation limits one to at most an octave of bandwidth anywhere within the frequency response of the modulator. Hence in an actual application, one would need some form of frequency-selective component or circuit before the modulator. In the case of the dual-drive modulator-based link, the 180-degree hybrid coupler can be a bandwidth-limiting component much like a filter. In antenna remoting applications, the antenna itself might provide frequency selectivity, whereas in applications where out-of-band signals must be suppressed by a factor greater than what the coupler and/or antenna can provide, a pre-selecting filter must be used. The loss of this filter in dB would add directly to the noise figure.

IV. Conclusions

Improving the performance of the devices that comprise a low-biased intrinsic fiber-optic link has yielded record low noise figure performance, with a minimum of 3.4 dB at 2 GHz, and a correspondingly high gain and *SFDR*. To achieve such low noise figures, it must be that we are at last approaching the condition where the dominant contributor to the link's output noise must be thermal noise generated in the input circuit, which includes the modulator's input interface circuitry, electrodes, and termination impedance. Future work at Photonic Systems, Inc. will be focused on carefully accounting for the effects of these thermal noise sources on the link noise figure.

References

[1] G. Betts, L. Johnson, and C. Cox, "High-sensitivity lumped-element bandpass modulators in $LiNbO_3$," *J. Lightwave Technol*., vol. 7, pp. 2078-2083, December 1989.

[2] E. Ackerman, C. Cox, G. Betts, H. Roussell, K. Ray, and F. O'Donnell, "Input impedance conditions for minimizing the noise figure of an analog optical link," *IEEE Trans. Microwave Theory Tech.,* vol. 46, pp. 2025-2031, December 1998.

[3] J. McKinney, M. Godinez, V. Urick, S. Thaniyavarn, W. Charczenko, and K. Williams, "Sub-10-dB noise figure in a multiple-GHz analog optical link," *IEEE Photon. Technol. Lett*., vol. 19, pp. 465-467.

[4] E. Ackerman, G. Betts, W. Burns, J. Campbell, C. Cox, N. Duan, J. Prince, M. Regan, and H. Roussell, "Signal-to-noise performance of two analog photonic links using different noise reduction techniques," *IEEE MTT-S Int. Microwave Symp. Dig.*, pp. 51-54, June 2007.

[5] A. Karim and J. Devenport, "Noise figure reduction in externally modulated analog fiber-optic links," *IEEE Photon. Technol. Lett*., vol. 19, pp. 312-314

[6] X. Li, N. Li, X. Zheng, S. Demiguel, J. Campbell, D. Tulchinsky, and K. Williams, "High-saturation-current InP/InGaAs photodiode with partially depleted absorber," *IEEE Photon. Tech. Lett*., vol. 15, pp. 1276-1278, 2003.

[7] X. Li, N. Li, S. Demiguel, J. Campbell, D. Tulchinsky, and K. Williams, "A comparison of frontside and backside illuminated high-saturation-power partially-depleted-absorber photodetectors," *IEEE J. Quantum Electron*., vol. 40, pp. 1321-1325, 2004.

[8] D. Pozar, Microwave Engineering, John Wiley & Sons, 2005.

[9] C. Cox, *Analog Optical Links*, Cambridge University Press, 2003.

[10] C. Cox, E. Ackerman, G. Betts, and J. Prince, "Limits on the performance of RF-over-fiber links and their impact on device design," *IEEE Trans. Microwave Theory Tech*., vol. 54, pp. 906-920, February 2006.

[11] H. Haus, *et al*., "IRE standards on methods of measuring noise in linear twoports, 1959," *Proc. IRE*, vol. 48, pp. 60-68, January 1959.